Supplementary Materials
Molecular Biology of the Cell
Perez-Vale *et al*.

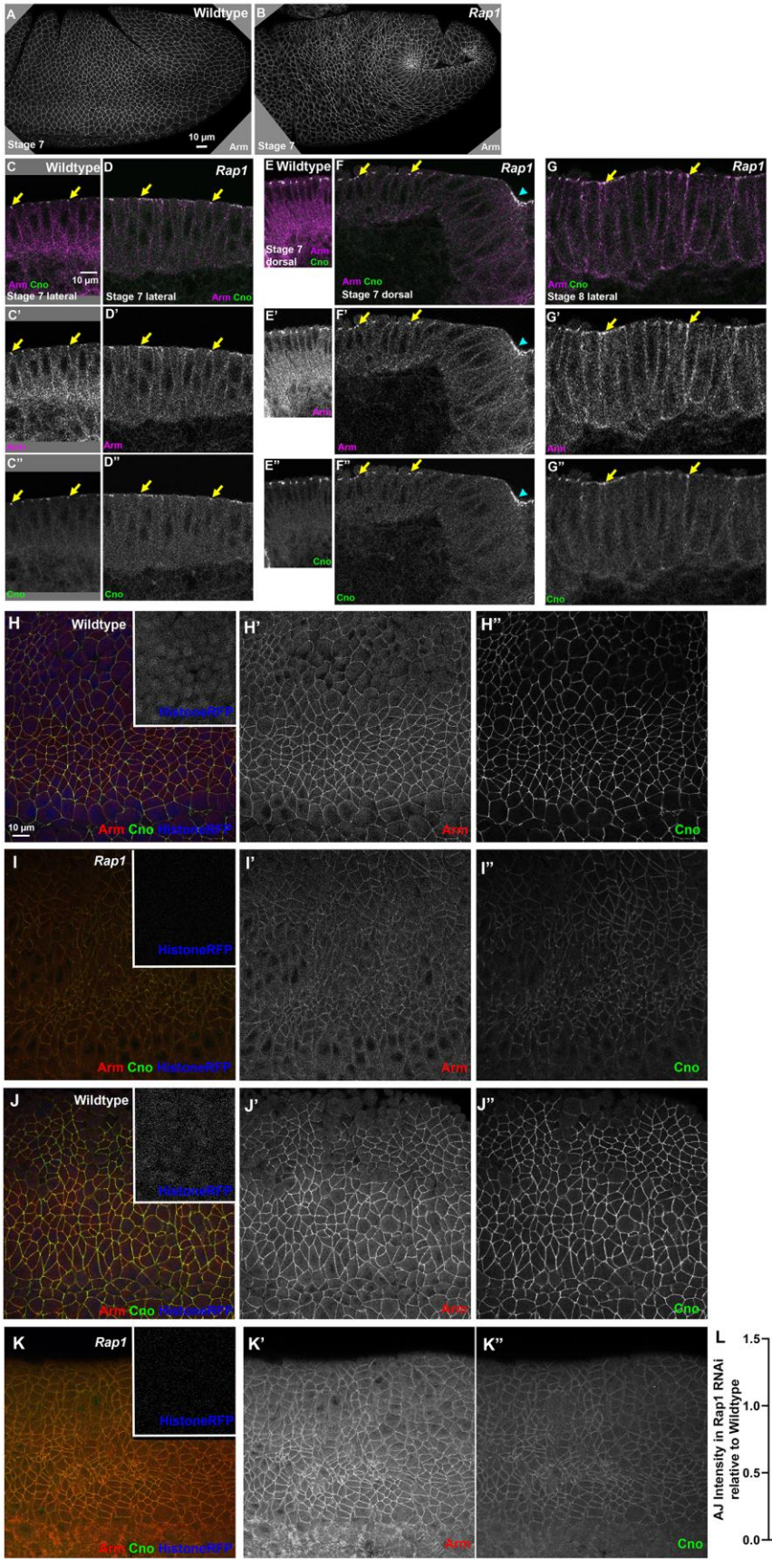
A
Wildtype
Stage 7
10 µm
Arm
B
Rap1
Stage 7
Arm
C
Wildtype
Arm Cno
10 µm
Stage 7 lateral
D
Rap1
Stage 7 lateral
Arm Cno
E Wildtype
Stage 7
dorsal
Arm
Cno
F
Rap1
Arm Cno
Stage 7 dorsal
G
Rap1
Arm Cno
Stage 8 lateral
C'
D'
E'
F'
G'
Arm
C''
D''
E''
F''
G''
Cno
H
Wildtype
HistoneRFP
10 µm
Arm Cno HistoneRFP
H'
Arm
H''
Cno
I
Rap1
HistoneRFP
Arm Cno HistoneRFP
I'
Arm
I''
Cno
J
Wildtype
HistoneRFP
Arm Cno HistoneRFP
J'
Arm
J''
Cno
K
Rap1
HistoneRFP
Arm Cno HistoneRFP
K'
Arm
K''
Cno
L
AJ Intensity in Rap1 RNAi
relative to Wildtype
1.5
1.0
0.5
0.0
Arm
Cno

Figure S1. Arm and Cno remain enriched in apical AJs after *Rap1* RNAi and Arm and Cno levels are reduced at AJs. A,B. Stage 7 embryos illustrating twisted gastrulation phenotype after *Rap1* RNAi. C-F. Stage 7 embryos. A-D. Arm and Cno remain enriched in apical AJs (arrows) after *Rap1* RNAi in both the lateral (C vs. D) and dorsal ectoderm (E vs. F). They also remain enriched in apical AJs of invaginating posterior midgut cells (F, arrowhead). G. Stage 8 embryo. Arm and Cno remain enriched in apical AJs (arrows) after *Rap1* RNAi. H-K. Wildtype embryos (marked with Histone:RFP) and *Rap1* RNAi embryos stained together in the same tube and visualized using the same confocal microscope settings. Embryos from two representative experiments are shown. L. Quantification of Arm and Cno levels at 12 bicellular junctions per embryo in five embryos, with cytoplasmic background subtracted, and normalized to wildtype embryos from the same experiment. Dots are average values at the 12 bicellular junctions in individual embryos, the bold line represents the mean for each genotype, and smaller lines represent the minimum and maximum range.

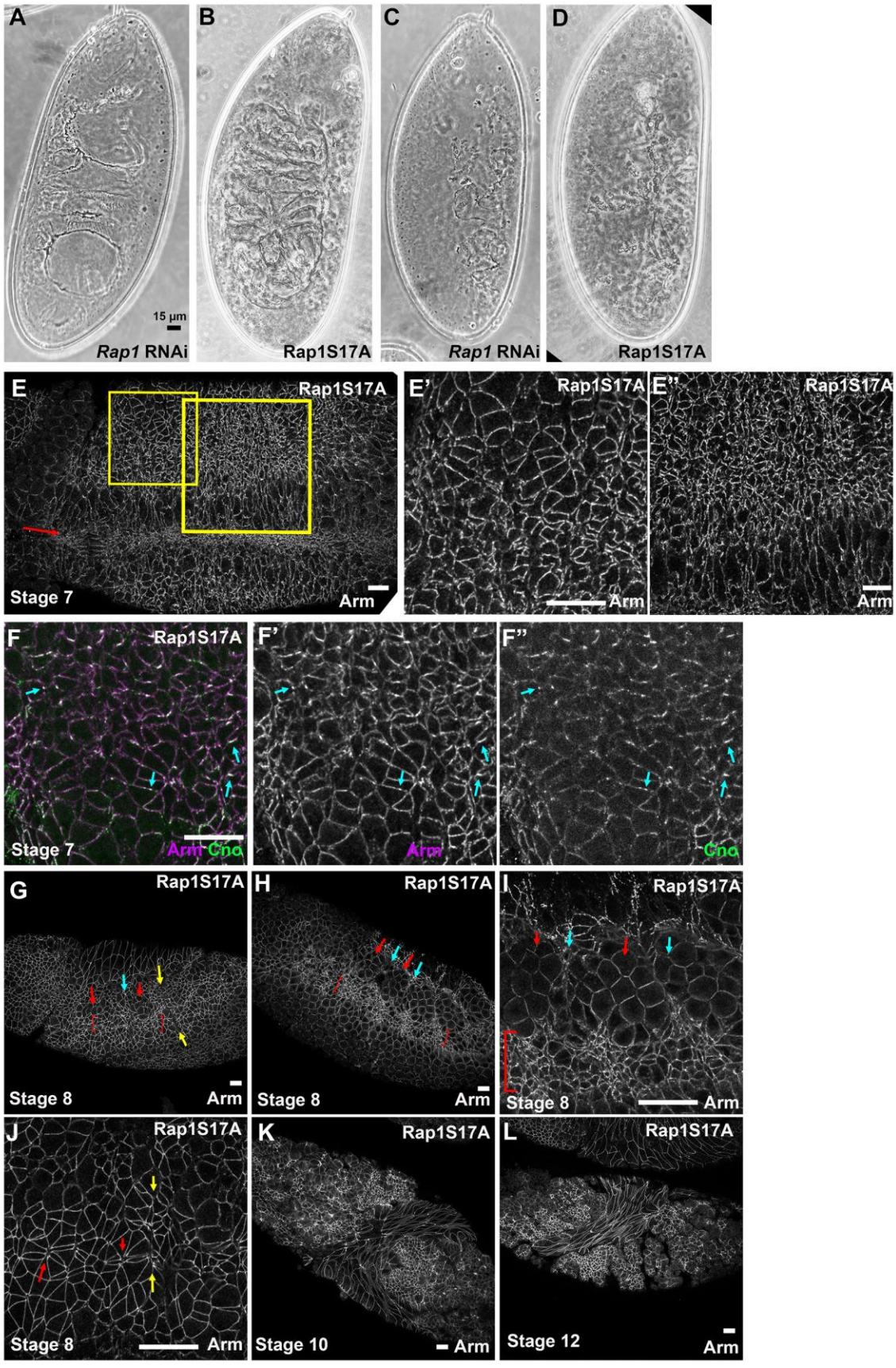
A
15 µm
Rap1 RNAi
B
Rap1S17A
C
Rap1 RNAi
D
Rap1S17A
E
Rap1S17A
Stage 7
Arm
E'
Rap1S17A
Arm
E''
Rap1S17A
Arm
F
Rap1S17A
Stage 7
Arm Cno
F'
Arm
F''
Cno
G
Rap1S17A
Stage 8
Arm
H
Rap1S17A
Stage 8
Arm
I
Rap1S17A
Stage 8
Arm
J
Rap1S17A
Stage 8
Arm
K
Rap1S17A
Stage 10
Arm
L
Rap1S17A
Stage 12
Arm

Fig. S2. Expressing the GDP-locked Rap1 dominant-negative mutant Rap1S17A mimics the effect of *Rap1*RNAi, verifying that these are not due to off-target effects. A-D. Cuticles (anterior up) of *Rap1* RNAi or Rap1S17A embryos share moderate (A, B) or strong (C, D) disruption of the epidermis. E, F. Stage 7 embryos expressing Rap1S17A, exhibiting phenotypes we also observed after *Rap1* RNAi. E. Areas in yellow boxes are enlarged in E' and E". Mesoderm invagination is blocked (red arrow) and apical AJs are strongly altered, with gaps (E') and reduced apical area (E"). F. In more basal sections, Cno localization becomes less continuous, and regions where Cno remains strong also have stronger localization of Arm (arrows). G-J. Stage 8 embryos expressing Rap1S17A, exhibit phenotypes we also observed after *Rap1* RNAi. G, J. Milder phenotypes. H, I. Stronger phenotypes. Brackets indicate hyperconstricted cells ventral to mitotic domains 11 (red arrows). Cells between the mitotic domains also hyperconstrict and sometimes fold inward (cyan arrows). J. Gaps at tricellular junctions and aligned AP borders (red arrows) and incipient folds (yellow arrows). K ,L. Later stage embryos expressing Rap1S17A, exhibiting the disrupted epidermis and deep folds also seen after *Rap1* RNAi. Scale bars = 15µm.

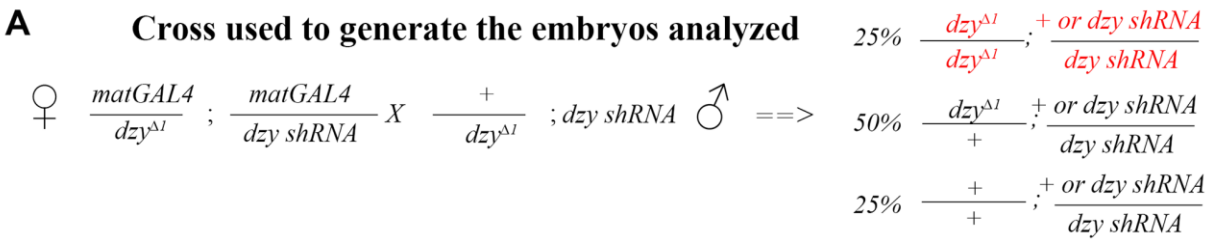

Figure S3. Genetic cross used to generate “dzy RNAi” embryos. We used the GAL4/UAS system to express an shRNA targeting dzy both maternally and zygotically. The use of the strong dual MatGAL4 driver ensures strong knockdown of maternal mRNA. 25% of the embryo are homozygous for the *dzy*$^{\Delta 1}$ null allele and thus have no zygotic gene expression—these should have the strongest knockdown of Dzy protein.

Table S1. **Number of cells analyzed for planar cell polarity**

Antigen	**Wildtype**	***dzy* RNAi**	***rap1* RNAi**
Armadillo	129	236	145
Bazooka	65	111	72
Canoe	64	125	73
Polychaetoid	64	125	73

Table S2. ***Drosophila*** **stocks used in this study**

Drosophila **Stock**	**Source**
dzy$^{\Delta 1}$/Cyo	Huelsmann et al., 2006
dzy shRNA	Created here—see Materials and Methods
y^{1} w^{67c23}; P{CaryP}attP2	Bloomington Drosophila Stock Center (Stock #8622)
Mat-tub-Gal4;Mat-tub-Gal4	Bloomington Drosophila Stock Center (stock #80361)
Ubi-Ecad:GFP sqh>myosin light chain–mCherry	J. Zallen (Sloan-Kettering, NY, USA)
UAS.Rap1 RNAi v20/TM3, Sb	Bloomington Drosophila Stock Center (stock no. 35047)

Table S3. **Antibodies used in this study**

Primaries	**Species**	**Dilution**	**Source**
Anti-Canoe	Rabbit IgG	1:1,000	Sawyer et al., 2009
Anti-Bazooka	Rabbit IgG	1:2,000	Choi et al., 2013
Anti-Armadillo (N27A1)	Mouse IgG_{2a}	1:100	Developmental Studies Hybridoma Bank
Anti-Polychaetoid (PYD2)	Mouse IgG_{2b}	1:500	Developmental Studies Hybridoma Bank
Anti-PKC ζ (C-20)	Rabbit IgG	1:2,000	Santa Cruz Biotechnology (SC-216)
Anti-Phospho-Histone H3	Mouse IgG_1	1:1,000	ProteinTech Group (66863-1-Ig)
Anti-Neurotactin	Mouse IgG_{2a}	1:500	Developmental Studies Hybridoma Bank

Secondary antibodies	**Dilution**	**Source**
Alexa Fluor 488, 568, 647	1:1,000	Life Technologies